DIABETES, OBESITY AND METABOLISM
A JOURNAL OF PHARMACOLOGY AND THERAPEUTICS

Regulation of hepatic glucose production and AMPK by AICAR but not metformin depends on drug uptake through the equilibrative nucleoside transporter 1 (ENT1)

Journal:	*Diabetes, Obesity and Metabolism*
Manuscript ID	DOM-18-0355-OP.R3
Manuscript Type:	Original Paper
Date Submitted by the Author:	28-Jun-2018
Complete List of Authors:	Logie, Lisa; University of Dundee, Cellular Medicine Lees, Zoe ; University of Dundee, Cellular Medicine; The James Hutton Institute, Invergowrie, Dundee. DD2 5DA, Scotland, UK., Environmental and Biochemical Sciences Allwood, William; The James Hutton Institute, Invergowrie, Dundee. DD2 5DA, Scotland, UK., Environmental and Biochemical Sciences. McDougall, Gordon; The James Hutton Institute, Invergowrie, Dundee. DD2 5DA, Scotland, UK., Environmental and Biochemical Sciences. Beall, Craig; University of Exeter, Institute of Biomedical and Clinical Sciences Rena, Graham; University of Dundee,
Key Words:	antidiabetic drug, cellular research, drug mechanism, glucose metabolism, metformin

Regulation of hepatic glucose production and AMPK by AICAR but not metformin depends on drug uptake through the equilibrative nucleoside transporter 1 (ENT1).

Lisa Logie[1], Zoe Lees[1, 2], J. William Allwood[2], Gordon McDougall[2], Craig Beall[3]*, Graham Rena[1]*

[1]Division of Cellular Medicine, Ninewells Hospital and Medical School, University of Dundee, Dundee, Scotland, UK. DD1 9SY

[2] Environmental and Biochemical Sciences, The James Hutton Institute, Invergowrie, Dundee. DD2 5DA, Scotland, UK.

[3]Institute of Biomedical & Clinical Science, University of Exeter Medical School, RILD Building (Level 4) Room 4.06, Barrack Road, Exeter. EX2 5DW

***Corresponding authors: c.beall@exeter.ac.uk; g.rena@dundee.ac.uk**

Keywords: AICAR, metformin, hepatocyte, hepatic glucose production, 8CPT-cAMP, AMPK, ENT1,

Abstract word count:

Main body word count: 3342

Tables: 0

Figures: 5

Abstract

Aim: Recently we have observed differences in the ability of metformin and AICAR to repress glucose production from hepatocytes using 8CPT-cAMP. Previous results indicate that besides activating protein kinase A, 8CPT-modified cAMP analogues suppress the Nitrobenzylthioinosine (NBMPR)-sensitive equilibrative nucleoside transporter ENT1. We aimed to exploit 8CPT-cAMP, 8CPT-2-Methyl-O-cAMP and NBMPR, which is highly selective for a high-affinity binding-site on ENT1, to investigate the role of ENT1 in the liver specific glucose lowering properties of AICAR and metformin.

Methods: Primary mouse hepatocytes were incubated with AICAR and metformin in combination with cAMP analogues, glucagon, forskolin and NBMPR. Hepatocyte glucose production (HGP), and AMPK signalling were measured and a uridine uptake assay with supporting LC-MS was used to investigate nucleoside depletion from medium by cells.

Results: AICAR and metformin increased AMPK pathway phosphorylation and decreased HGP induced by dibutyryl cAMP and glucagon. HGP was also induced by 8CPT-cAMP, 8CPT-2-Methyl-O-cAMP and NBMPR; however, in each case this was resistant to suppression by AICAR but not metformin. Cross-validation of tracer and mass spectrometry studies indicates that 8CPT-cAMP, 8CPT-2-Methyl-O-cAMP and NBMPR inhibited the effects of AICAR at least in part by impeding its uptake into hepatocytes.

Conclusions: We report for the first time that suppression of ENT1 induces HGP. ENT1 inhibition also impedes uptake and effects of AICAR but not metformin on HGP. Further investigation of nucleoside transport may illuminate a better understanding of how metformin and AICAR each regulate HGP.

Introduction

Stimuli that raise cyclic adenosine monophosphate (cAMP) levels in hepatocytes, including glucagon, induce *de novo* glucose production through gluconeogenesis and from glycogenolysis (1). Hyperglucagonaemia contributes to chronic hyperglycaemia observed in type 1 (T1D) and type 2 diabetes (T2D), through poorly defined mechanisms. Raised intracellular cAMP activates downstream effectors including cAMP-dependent protein kinase (PKA) (1; 2) to control gluconeogenic flux through the actions of PKA on fructose-1,6-bisphosphatase. Phosphorylation of cAMP-response element binding protein (CREB) by PKA is believed to contribute towards gluconeogenesis through increased expression of phosphoenolpyruvate carboxykinase (PEPCK) and glucose-6-phosphatase (G6-Pase).

The hyperglycaemic effect of the glucagon/cAMP/PKA signalling pathway on liver cells has been studied using a number of different cAMP analogues, in combination with dexamethasone, to stimulate cAMP/PKA (3-5). Commonly used is the cAMP analogue dibutyryl cAMP (bucladesine, db-cAMP), a cell permeable stabilised cAMP mimic which also inhibits phosphodiesterase (PDE) activity (6; 7). Treatment of cells with db-cAMP causes a significant stimulation of PEPCK and G6-Pase expression, which is inhibited by the addition of insulin in a dose-dependent manner (8-10). 8-(4-Chlorophenylthio)cAMP (8CPT-cAMP), like db-cAMP, is a membrane permeable cAMP analogue that stimulates PEPCK and G-6-Pase (4; 11); tends to be more potent than cAMP; is more resistant to phosphodiesterase-dependent hydrolysis and it acts as a PDE inhibitor (12).

Studies using cAMP analogues have previously shown that the type 2 diabetes drug metformin and 5-Aminoimidazole-4-carboxamide ribonucleoside (AICAR) repress cAMP-stimulated hepatocyte glucose production (HGP) (13-15). Inside cells, AICAR

is phosphorylated by adenosine kinase to form ZMP, which then acts as mimic of AMP to activate AMPK (16). Metformin and AICAR are both activators of AMPK; however earlier studies including some carried out in mice where the catalytic subunits of AMPK are genetically ablated, demonstrated that suppression of HGP occurs independently of AMPK activation (13-15; 17; 18). Metformin is transported across hepatocyte cell membranes, at least in part, by organic cation transporter (OCT) family of transporters (18-20). Previous studies using siRNA determined that AICAR is transported by ENT1 and CNT3 into human macrophages (21), whereas AICAR uptake into hepatocytes and the role on HGP is less clear. Initiating the current investigation, we observed that HGP was highly resistant to inhibition by AICAR only when 8CPT-modified cAMP analogues were used to stimulate HGP. In contrast, repression of HGP by metformin was unaffected. 8CPT-modified cAMP analogues have previously been shown to inhibit the equilibrative nucleoside transporter (ENT1), which is expressed in the liver (22) and transports nucleosides across the plasma membrane depending upon the nucleoside concentration gradient (23). The inhibitory effect of 8CPT-modified cAMP analogues on AICAR action prompted us to investigate the role of ENT1 in metformin and AICAR-induced regulation of HGP using NBMPR, a highly selective ENT1 inhibitor (24). Our study indicates that suppression of ENT1 activity is sufficient to induce HGP. Moreover, the effects of AICAR but not metformin on HGP are sensitive to ENT1 inhibition. These data highlight direct and indirect roles for ENT1 in modulating HGP.

Materials and methods

Materials

AICAR and 4-Nitrobenzylthioinosine (NBMPR) were purchased from Tocris, dibutyryl cAMP, uridine and metformin were from Sigma (Dorset, UK). LC-MS materials were obtained from Fisher Scientific unless otherwise stated. Glucagon was from Novo Nordisk (Bagsvaerd, Denmark). 8CPT-cAMP was purchased from Calbiochem and 8CPT-2-Methyl-O-cAMP (8CPT-2MeO-cAMP) was from Biolog Life Sciences Institute (Bremen, Germany). Donkey anti-goat 680RD, donkey anti-mouse 680RD, donkey anti-rabbit 800CW secondary antibodies were purchased from LI-COR Biosciences, UK. GAGO glucose oxidase kit was purchased from Sigma. [5,6-^{3}H] Uridine was purchased from Perkin Elmer. pAMPK (Thr172) and total ACC antibodies were from Cell Signalling Technologies. Total AMPK was purchased from Abcam, actin was from Proteintech and pACC was made in-house by DSTT (University of Dundee).

Isolation of mouse primary hepatocytes

Hepatocytes were isolated from adult female mice essentially as described by Foretz et al (14) and in accordance with the Animals (Scientific Procedures) Act 1986. Following successful isolation, cell viability was determined by 0.04% Trypan blue staining and the cell number determined using a haemocytometer. Cell viability of >90% was required before experimental use. Cells were plated at a density of $2.5x10^{5}$ cells per ml for all experiments.

Measurement of Hepatocyte glucose production (HGP) from primary cells

HGP was measured essentially as previously described (25) using mouse primary hepatocytes. Viable cells were allowed to settle for 4-6 hours before serum starvation in M199 media containing dexamethasone (100 nM). After overnight serum free conditions, cells were washed once in PBS before incubation for 8 hours in glucose free DMEM (Invitrogen) containing lactate (10 mM), pyruvate (1 mM), dexamethasone (100 nM) plus stimuli as indicated on the figure legends. Media was harvested for measurement of glucose and hepatocytes were lysed. The amount of glucose present in the media was measured using GAGO glucose oxidase kit (Sigma). Glucose assays were performed in a 96-well plate format. 50 µl of cell culture media was incubated with 100 µl of glucose oxidase/peroxidase assay reagent for 30 minutes at 37^{o}C before the reaction was stopped by the addition of 100 µl 12N H_2SO_4. Absorbance was measured at 405 nm and the amount of glucose present was determined using a glucose standard curve generated in the same assay. The final glucose concentration was normalized to total protein content per well and data is presented as µg HGP per µg protein.

Cell lysis and Western blotting

Cells were lysed in buffer containing Tris-HCl (50 mM; pH7.4), NaF (50 mM), sodium pyrophosphate (1 mM), EDTA (1 mM), EGTA (1 mM), NaCl (50 mM), sucrose (0.27 M), 1% (v/v) Triton-X100, 0.1% (v/v) 2-mercaptoethanol, sodium orthovanadate (1 mM), benzamidine (1mM) and 0.1% (v/v) pefabloc (a serine protease inhibitor). Cells were allowed to lyse on ice for 30 minutes before scraping. Lysates were centrifuged at 13K rpm for 15 minutes at, 4°C and prepared in 1x LDS (final) plus DTT (10 mM). Gels were run at 150V for 90 minutes and transferred onto nitrocellulose (GE healthcare) for 3 hours at 75V before blocking in 1% (w/v) BSA,

TBS-T for 30 minutes at room temperature. Membranes were incubated with primary antibodies diluted 1:1000 except actin, which was diluted 1:5000 as indicated in the figure legends at 4°C overnight with shaking before washing 3x10 minutes in 1xTBS-T. Secondary antibodies (LI-COR Biosciences, UK) were added at 1:5000 for 1 hour at room temperature with shaking. Protein bands were visualized using LI-COR Odyssey infra-red imaging system.

Uridine Uptake Assay

Primary mouse hepatocytes were incubated overnight in M199 media as described above. Cells were washed once in uridine uptake buffer (20 mM Tris-HCl, 3 mM KH_2PO_4, 1 mM $MgCl_2.6H_2O$, 2 mM $CaCl_2$, 5 mM Glucose, 130 mM NaCl, pH7.4) before incubating at room temperature in 400 µl uridine uptake buffer containing either DMSO (0.1% v/v), NBMPR (100 nM), 8CPT-cAMP (100 µM), 8CPT-2MeO-cAMP (100 µM), db-cAMP (100 µM) or glucagon (100 nM). After 15 minutes, 400 µl uridine uptake buffer containing compounds plus 0.1 µM (2 µCi/ml) ^{3}H-uridine was added. After 1 minute, uridine transport was stopped by washing cells five times in ice cold uridine uptake buffer containing cold uridine (1 mM). Cells were lysed in 200 µl 10% (w/v) SDS before scraping. The amount of uridine taken into the cell was determined by scintillation counting. Data is represented as percentage uptake compared with untreated control.

Liquid Chromatography – Mass Spectrometry (LC-MS) analysis

Samples of culture media were transferred into 300 µl micro-vials and capped (PN 60180-507 and PN 60180-516; Thermo Scientific, Hemel Hempstead, UK). LC-MS analysis was performed with a Thermo Accela 600 HPLC system coupled with an

Accela PDA detector (Thermo-Fisher Ltd. Hemel Hempstead, UK). The samples were stored in the autosampler at 6 °C and analysed within 24 h of preparation. The HPLC flow rate was 300 µL/min and the column (Gemini C6-Phenol 110Ä, 150 x 2 mm, 5 µm particle size; Phenomenex Ltd. Macclesfield, U.K.) was maintained at a temperature of 30 ºC. Solvent A was 5 mM ammonium acetate in deionised water (ELGA-PureLab option-Q, Elga Ltd, High Wycombe U.K.) adjusted to pH 3.5 with acetic acid and solvent B was HPLC grade acetonitrile (Fisher Scientific Ltd, Loughborough, UK). Prior to sample analysis, the column was conditioned with solvents A and B for 40 min. Samples (10 µL) were injected and eluted on a gradient programme of 100% A from 0-2 min, 100 - 95% A over 2-5 min, 95 - 55% A from 5 - 25 min, 55% A - 100% B over 25 - 26 min, hold 100% B over 26-29 min, then 100% B – 100% A over 29-30 min, hold 100% A from 30-35 min. HPLC needle washes were performed with 8:2 acetonitrile:water. The Accela PDA detector collected spectra from 200-600 nm and monitored channels at 280, 365 and 520 nm.

The PDA detector eluent was next transferred to a Thermo LTQ-Orbitrap XL mass spectrometry system operated under Xcalibur software (Thermo-Fisher Ltd). For the first 3 minutes, the HPLC eluent flow was directed to waste, then from 3 to 35 min to the FT-MS detector. Mass spectra were collected in full scan mode (*m/z* 80-2000) at a mass resolution of 30,000 in both positive and negative ESI modes, although positive mode provided the greatest sensitivity for AICAR. A second method was employed to validate compound identification through retention time and MS2 spectral matching to the reference standard. Here, data-dependent MS2 CID fragmentation spectra (Acquisition-Q 0.25, Activation time 25ms, Normalised Collision Energy 10 - optimised for AICAR and metformin) were collected in the LTQ for the three most intense ions as defined within the preliminary full FT-MS scan.

Both scan events generated 'centroid' spectral data. Scan speeds of 0.1 seconds and 0.4 seconds were applied in the LTQ and FT-MS respectively. The Automatic Gain Control was set to $1x10^5$ and $5x10^5$ for the LTQ and FT-MS respectively. The ESI settings were optimised to allow efficient ionisation and ion transmission with low in-source fragmentation; spray voltage +4.5kV; sheath gas 60; auxiliary gas 20; capillary voltage +10V; tube lens voltage +80V and capillary temperature at 280ºC.

The MS detector was calibrated according to the manufacturer's instructions then tuned to optimise detection of ions in the mid *m/z* 80-2000 range. All samples were run in a randomised order, with control and blank samples interspersed every 6 analyses and at the start and end of the run to monitor the HPLC-MS background and target compound carryover.

A stock solution of 750 μM AICAR (99%+ pure; Sigma Chemical Co. Ltd) was prepared in fresh culture media (Dulbecco's Modified Eagle Medium 1X, Gibco Life Technologies Corp., Paisley, UK), then serially diluted in culture media to provide calibration standard curves. Extracted ion chromatograms for AICAR were generated within the Xcalibur Qual Browser software, peak areas were extracted applying the GENESIS peak detection algorithm and the raw extracted peak areas were transferred to Microsoft Excel.

Statistics

All statistical analysis was performed using GraphPad Prism version 6.0. Mean glucose values were taken from each experiment and in one experiment normalised to control, which was set at 100% to account for variability between different hepatocyte preparations. HGP and western blotting data were analysed by ANOVA.

For the Uridine uptake assay, data was expressed as percentage of control uptake and analysed by one sample t-test with control set to 100%.

Results

8CPT-cAMP inhibits AICAR but not metformin repression of HGP.

Primary mouse hepatocytes were serum starved overnight before incubating with 8CPT-cAMP (100 μM) in the presence or absence of AICAR (250 μM) or metformin (250 μM) for 8 hours. Consistent with previous work (26), incubation of hepatocytes with 8CPT-cAMP increased HGP. AICAR (250 μM) caused an almost complete inhibition of basal but not 8CPT-cAMP-stimulated HGP suggesting that 8CPT-cAMP interferes with the ability of AICAR to inhibit HGP. In contrast, even though metformin (250 μM) caused only a modest repression of basal HGP, it significantly repressed 8CPT-cAMP stimulated HGP (Fig. 1A). Metformin and AICAR both activate AMPK. Previous work, including experiments where AMPK activity was genetically ablated, indicate that AMPK is not essential for regulation of HGP, even though both drugs activate AMPK (13-15; 17; 18). In the current study we used AMPK activation purely as a marker of drug entry into the cell. 8CPT-cAMP prevented increases in phosphorylation of acetyl CoA carboxylase (ACC) and AMPK by AICAR but not metformin (Fig. 1B-D) indicating that activation of the AMPK signalling pathway by AICAR was selectively blocked by 8CPT-cAMP.

Inhibition of AICAR's effects depends on the 8CPT moiety of 8CPT-cAMP.

We investigated the ability of AICAR to suppress HGP in the presence of db-cAMP and glucagon to induce endogenous cAMP. In contrast to 8CPT-cAMP, AICAR significantly repressed HGP in the presence of db-cAMP (100 μM; Fig. 2A) and glucagon (100 nM; Fig. 2B). In addition, effects of AICAR on AMPK and ACC phosphorylation were not modified by db-cAMP and glucagon, (Fig. 2C-E). AICAR

also suppressed HGP induced by the adenylate cyclase activator forskolin (100 μM, supporting material Fig. 1).

To determine whether other 8CPT-modified cAMP analogues inhibit the effect of AICAR on HGP and AMPK signalling, we utilised 8CPT-2MeO-cAMP. We incubated primary mouse hepatocytes with 8CPT-2MeO-cAMP and found that similarly to 8-CPT-cAMP, 8CPT-2MeO-cAMP blocked repression of HGP by AICAR (Fig. 3A). When the effects of 8CPT-2MeO-cAMP on AMPK and ACC phosphorylation were studied, we found that like 8CPT-cAMP, 8CPT-2MeO-cAMP selectively inhibited AICAR but not metformin's ability to stimulate AMPK signalling (Fig. 3B-F).

AICAR uptake into hepatocytes is mediated by equilibrative nucleoside transporter 1 (ENT1).

Previous studies have shown that 8-CPT modified cAMP analogues are potent inhibitors of the equilibrative nucleoside transporter 1 (ENT1) (23), which in brain slices was previously found to mediate AICAR uptake (27). This led us to test whether AICAR uptake into hepatocytes may be blocked by inhibition of ENT1. We incubated primary mouse hepatocytes with AICAR and metformin in the presence of the selective ENT1 inhibitor NBMPR (Fig. 4A). This compound was sufficient to promote HGP alone but completely blocked the action of AICAR on HGP (Fig. 4B). The effect of metformin on AMPK and ACC phosphorylation was not modified by the presence of NBMPR (Fig. 4B-D), whereas AICAR failed to alter AMPK or ACC phosphorylation in the presence of NBMPR (Fig. 4B, E, F). These data strongly suggest that AICAR uptake into mouse hepatocytes is mediated by ENT1. To confirm that 8CPT-cAMP and 8CPT-2MeO-cAMP inhibit ENT1 in hepatocytes, we performed an uptake assay using radiolabelled uridine as a tracer and a known

ENT1 substrate, to measure ENT1 activity in the absence and presence of NBMPR, 8CPT-cAMP, 8CPT-2MeO-cAMP, db-cAMP and glucagon. We found that ^{3}H-uridine uptake was inhibited by NBMPR, 8CPT-cAMP and 8CPT-2MeO-cAMP but not by db-cAMP or glucagon (Fig. 5). To reinforce these findings, we carried out LC-MS analysis of AICAR depletion from cellular medium. A scan of the cell culture medium without AICAR is presented in Supplementary Fig 2A. On the same column, AICAR, ran as a single peak at 2.91 minutes (Supplementary Fig 2B-D). We then established that AICAR added to the medium alone was stable up to 24 hours, with LC-MS traces superimposable (Fig 5B; 0 minutes versus 360 mins), indicating that AICAR is not degraded over this time-period. When compared with media harvested from cells treated with AICAR, we observed AICAR loss from the medium (Fig. 5C), which was blocked by NBMPR, 8CPT-cAMP and 2MeO-8CPT-cAMP (Fig. 5D).

Discussion

Regulating HGP is key to maintaining adequate blood glucose control in T1 and T2 diabetes. Glucagon and a number of cAMP analogues including 8CPT-cAMP and db-cAMP are used in pre-clinical studies to mimic HGP in the fasted state, allowing liver specific effects of metformin and AICAR on HGP to be studied *in vitro*.

This study was initiated by our observation that 8CPT-cAMP selectively blocks suppression of HGP and activation of AMPK signalling in response to AICAR but not metformin. Db-cAMP and glucagon stimulated HGP, which was reversed by AICAR. A second 8CPT-modified analogue, 8CPT-2MeO-cAMP produced a similar selective block of the effect of AICAR on both HGP and AMPK signalling. Earlier investigations found that 8CPT-cAMP and 8CPT-adenosine did not inhibit the binding of [^{3}H]NBMPR to PC12 cells (23) and consequently the mechanism of 8CPT-cAMP/8CPT-adenosine dependent inhibition of ENT1 is uncertain but likely to be related to 8CPT-cAMP being greater than one order of magnitude more lipophilic than cAMP (28). This significant off-target effect of 8CPT-modified cAMP analogues suggests that caution should be exercised in future studies using 8CPT-cAMP to stimulate HGP. In the current study however, we exploited this action of 8CPT-modified cAMP analogues to compare hepatic actions of AICAR and metformin.

We excluded a role for PKA/Epac activation in the blocking effect of 8CPT-modified cAMP analogues on AICAR-dependent suppression of HGP, on the basis that cAMP does not affect the inhibitory effect of AICAR on HGP (raised by the physiological inducer of cAMP, glucagon and by the adenylate cyclase activator forskolin). Importantly, it has previously been reported that 8CPT-modified cAMP analogues inhibit nucleoside transporters (23), which are divided into two different families; constitutive nucleoside transporters - CNT (SLC28) of which there are 3 members

(CNT1-3) or equilibrative nucleoside transporters ENT (SLC29) of which there are 4 members (ENT1-4, (29)). These nucleoside transporters are responsible for transporting nucleosides such as adenosine and uridine into the cell. In the brain, AICAR elevates adenosine levels, thought to be mediated by competition for or blockade of ENT1 (27). Therefore we used a highly selective inhibitor of ENT1, NBMPR, to demonstrate that ENT1 inhibition is sufficient to block the effect of AICAR on HGP and AMPK signalling. Molecular docking data is unavailable for 8CPT-cAMP analogues docking to ENT1 but in contrast, robust 3D-Quantitative Structure-Activity Relationship analysis is available for NBMPR/ENT1 interaction (30-32). NBMPR did not alter effects of metformin on AMPK and HGP. At the nanomolar concentrations used in the current study, NBMPR is highly specific for ENT1, which contains a unique high-affinity binding site for this drug (24). In recombinant systems, NBMPR inhibits ENT1 7000 fold more potently than ENT2 (24; 33) and it does not inhibit CNT3 (34). In rat hepatic membrane preparations, NBMPR is without effect on Na^+-dependent (concentrative) adenosine transport activity (35). To further validate that AICAR was taken up via ENT1, we used ^{3}H-uridine as a tracer. We confirmed that 8CPT-cAMP analogues and NBMPR inhibit uridine uptake into hepatocytes. We then cross-validated with LC-MS, demonstrating that AICAR is depleted from media harvested from AICAR-treated hepatocytes, which was prevented by NBMPR and 8CPT-modified cAMP analogues. As an additional control, we did not observe any major degradation products of AICAR in the medium, indicating that AICAR depletion is most likely due to cellular uptake. The difference between AICAR and metformin sensitivity to NBMPR is consistent with metformin being taken into the cell via OCT transporters as reported previously (19; 20). Our findings may explain previous observations that required the use of very high (2 mM) concentrations of AICAR to

inhibit 8CPT-cAMP induced HGP (11). Taken together our data suggest that 8CPT-modified cAMP analogues and NBMPR inhibit ENT1 to block AICAR entry, preventing AICAR-mediated inhibition of HGP and activation of AMPK (Fig 5E).

Direct ENT1 inhibition with NBMPR, which in other tissues raises extracellular adenosine levels (36; 37), was sufficient to increase HGP (Fig. 5E). This is likely mediated indirectly by activation of adenosine receptor-mediated glycogenolysis or gluconeogenesis (38). In addition to adenosine, ENT1 also transports uridine, which promotes feeding via activation of hypothalamic uridine diphosphate receptor, P2Y6 (39) and which may also contribute AMPK-independent effects of AICAR on metabolism. Several clinically used drugs inhibit ENT1 as a secondary mode of action, including rosuvastatin (40) and dipyridamole (41). Interestingly, rosuvastatin increases HbA1c in people with and without diabetes (42) and dipyridamole increases glycaemia in mice (43). Taken together, these data suggest that therapeutic alterations in purine salvage may produce a clinically significant alteration in HGP via modulation of adenosine receptors.

In summary, we report for the first time that suppression of ENT1 induces HGP. ENT1 inhibition also impedes uptake and effects of AICAR but not metformin on HGP. These data delineate differing pathways used by AICAR and metformin to regulate HGP and more study is required to determine whether exploitation of these pathways can be used for therapeutic intervention in diabetes.

Author contributions

L.L. performed all studies except LCMS carried out by Z.L. and directed by W.A. and G.M.. L.L., C.B. and G.R. designed the rest of the studies and interpreted data. G.R. and C.B. conceived the study. G.R. had access to all the data and is guarantor of the data.

Conflict of Interest

The authors have no conflict of interest to declare.

Acknowledgements

L.L. was supported by a Cunningham Trust PhD studentship awarded to G.R. and C.B. G.R. acknowledges additional support from the MRC (MR/K012924/1). This work was part-funded by a Tenovus Scotland grant to C.B, who is a recipient of a Diabetes UK RD Lawrence Fellowship (13/0004647). We wish to thank Dr Amy Cameron for obtaining preliminary data for this study and Prof. Rory McCrimmon, Jennifer Gallagher and Dr Alison McNeilly for supplying the mice for this study.

REFERENCES

1. Jiang G, Zhang BB. 2003. Glucagon and regulation of glucose metabolism. *American Journal of Physiology - Endocrinology And Metabolism* 284:E671-E8
2. Lin HV, Accili D. 2011. Hormonal Regulation Of Hepatic Glucose Production In Health And Disease. *Cell Metabolism* 14:9-19
3. Argaud D, Zhang Q, Pan W, Maitra S, Pilkis SJ, Lange AJ. 1996. Regulation of rat liver glucose-6-phosphatase gene expression in different nutritional and hormonal states: gene structure and 5'-flanking sequence. *Diabetes* 45:1563-71
4. Beebe SJ, Koch SR, Chu DTW, Corbin JD, Granner DK. 1987. Regulation of Phosphoenolpyruvate Carboxykinase Gene Transcription in H4IIE Hepatoma Cells: Evidence for a Primary Role of the Catalytic Subunit of 3′,5′-Cyclic Adenosine Monophosphate-Dependent Protein Kinase. *Molecular Endocrinology* 1:639-47
5. Cameron AR, Logie L, Patel K, Erhardt S, Bacon S, et al. 2018. Metformin selectively targets redox control of complex I energy transduction. *Redox Biology* 14:187-97
6. Henion WF, Sutherland EW, Posternak T. 1967. Effects of derivatives of adenosine 3′,5′-phosphate on liver slices and intact animals. *Biochimica et Biophysica Acta (BBA) - General Subjects* 148:106-13
7. Jarett L, Smith RM. 1974. Mode of Action of N6-O2′-Dibutyryl Cyclic 3′, 5′ AMP on Fat Cell Metabolism. *Diabetes* 23:29-40
8. Schmoll D, Wasner, C., Hinds, C.J., Allan, B.B., Walther, R., Burchell, A. 1999. Identification of a cAMP response element within the glucose- 6-phosphatase hydrolytic subunit gene promoter which is involved in the transcriptional regulation by cAMP and glucocorticoids in H4IIE hepatoma cells. *Biochem. J.* 338:457-63
9. Schmoll D, Walker KS, Alessi DR, Grempler R, Burchell A, et al. 2000. Regulation of glucose-6-phosphatase gene expression by protein kinase B alpha and the forkhead transcription factor FKHR - Evidence for insulin response unit-dependent and -independent effects of insulin on promoter activity. *J. Biol. Chem.* 275:36324-33
10. Granner D, Andreone T, Sasaki K, Beale E. 1983. Inhibition of transcription of the phosphoenolpyruvate carboxykinase gene by insulin. *Nature* 305:549-51
11. Lochhead PA, Salt IP, Walker KS, Hardie DG, Sutherland C. 2000. 5-aminoimidazole-4-carboxamide riboside mimics the effects of insulin on the expression of the 2 key gluconeogenic genes PEPCK and glucose-6-phosphatase. *Diabetes* 49:896-903
12. Miller JP, Boswell KH, Muneyama K, Simon LN, Robins RK, Shuman DA. 1973. Synthesis and biochemical studies of various 8-substituted derivatives of guanosine cyclic-3',5' phosphate, inosine cyclic-3',5' phosphate, and xanthosine cyclic-3',5' phosphate. *Biochemistry* 12:5310-9
13. Hasenour CM, Ridley DE, Hughey CC, James FD, Donahue EP, et al. 2014. 5-Aminoimidazole-4-carboxamide-1-beta-D-ribofuranoside (AICAR) effect on glucose production, but not energy metabolism, is independent of hepatic AMPK in vivo. *J. Biol. Chem.* 289:5950-9
14. Foretz M, Hébrard S, Leclerc J, Zarrinpashneh E, Soty M, et al. 2010. Metformin inhibits hepatic gluconeogenesis in mice independently of the

LKB1/AMPK pathway via a decrease in hepatic energy state. *J. Clin. Invest.* 120:2355-69

15. Rena G, Pearson ER, Hardie DG. 2017. The mechanisms of action of metformin. *Diabetologia* 60:1577-85
16. Corton JM, Gillespie JG, Hawley SA, Hardie DG. 1995. 5-Aminoimidazole-4-Carboxamide Ribonucleoside. *European Journal of Biochemistry* 229:558--65
17. Guigas B, Bertrand L, Taleux N, Foretz M, Wiernsperger N, et al. 2006. 5-Aminoimidazole-4-Carboxamide-1-β-d-Ribofuranoside and Metformin Inhibit Hepatic Glucose Phosphorylation by an AMP-Activated Protein Kinase–Independent Effect on Glucokinase Translocation. *Diabetes* 55:865-74
18. Rena G, Pearson ER, Sakamoto K. 2013. Molecular Mechanism of Action of Metformin: Old or New Insights? *Diabetologia* 56:1898-906
19. Shu Y, Sheardown SA, Brown C, Owen RP, Zhang S, et al. 2007. Effect of genetic variation in the organic cation transporter 1 (OCT1) on metformin action. *J. Clin. Invest.* 117:1422–31
20. Zhou K, Donnelly LA, Kimber CH, Donnan PT, Doney ASF, et al. 2009. Reduced-function SLC22A1 polymorphisms encoding organic cation transporter 1 and glycemic response to metformin: A GoDARTS study. *Diabetes* 58:1434-9
21. Boß M, Newbatt Y, Gupta S, Collins I, Brüne B, Namgaladze D. 2016. AMPK-independent inhibition of human macrophage ER stress response by AICAR. *Scientific Reports* 6:32111
22. Zimmerman MA, Tak E, Ehrentraut SF, Kaplan M, Giebler A, et al. 2013. Equilibrative nucleoside transporter (ENT)-1-dependent elevation of extracellular adenosine protects the liver during ischemia and reperfusion. *Hepatology (Baltimore, Md.)* 58:1766-78
23. Waidmann O, Pleli T, Dvorak K, Baehr C, Mondorf U, et al. 2009. Inhibition of the Equilibrative Nucleoside Transporter 1 and Activation of A2A Adenosine Receptors by 8-(4-Chlorophenylthio)-modified cAMP Analogs and Their Hydrolytic Products. *J. Biol. Chem.* 284:32256-63
24. Ward JL, Sherali A, Mo Z-P, Tse C-M. 2000. Kinetic and Pharmacological Properties of Cloned Human Equilibrative Nucleoside Transporters, ENT1 and ENT2, Stably Expressed in Nucleoside Transporter-deficient PK15 Cells: ENT2 exhibits a low affinity for guanosine and cytidine but a high affinity for inosine. *J. Biol. Chem.* 275:8375-81
25. Cameron AR, Morrison V, Levin D, Mohan M, Forteath C, et al. 2016. Anti-inflammatory effects of metformin irrespective of diabetes status. *Circ. Res.* 119:652-65
26. Cook JR, Matsumoto M, Banks AS, Kitamura T, Tsuchiya K, Accili D. 2015. A Mutant Allele Encoding DNA Binding–Deficient FoxO1 Differentially Regulates Hepatic Glucose and Lipid Metabolism. *Diabetes* 64:1951-65
27. Gadalla AE, Pearson T, Currie AJ, Dale N, Hawley SA, et al. 2004. AICA riboside both activates AMP-activated protein kinase and competes with adenosine for the nucleoside transporter in the CA1 region of the rat hippocampus. *Journal of Neurochemistry* 88:1272-82
28. Werner K, Schwede F, Genieser H-G, Geiger J, Butt E. 2011. Quantification of cAMP and cGMP analogs in intact cells: pitfalls in enzyme immunoassays for cyclic nucleotides. *Naunyn-Schmiedeberg's Archives of Pharmacology* 384:169

29. Baldwin SA, Beal PR, Yao SYM, King AE, Cass CE, Young JD. 2004. The equilibrative nucleoside transporter family, SLC29. *Pflügers Archiv* 447:735-43
30. Zhu Z, Buolamwini JK. 2008. Constrained NBMPR Analogue Synthesis, Pharmacophore Mapping and 3D-QSAR Modeling of Equilibrative nucleoside Transporter 1 (ENT1) Inhibitory Activity. *Bioorganic & Medicinal Chemistry* 16:3848-65
31. Gupte A, Buolamwini JK. 2009. CoMFA and CoMSIA 3D-QSAR studies on S6-(4-nitrobenzyl)mercaptopurine riboside (NBMPR) analogs as inhibitors of human equilibrative nucleoside transporter 1 (hENT1). *Bioorganic & Medicinal Chemistry Letters* 19:314-8
32. Zhu Z, Furr J, Buolamwini JK. 2003. Synthesis and Flow Cytometric Evaluation of Novel 1,2,3,4-Tetrahydroisoquinoline Conformationally Constrained Analogues of Nitrobenzylmercaptopurine Riboside (NBMPR) Designed for Probing Its Conformation When Bound to the es Nucleoside Transporter. *Journal of Medicinal Chemistry* 46:831-7
33. Yao SYM, Ng AML, Cass CE, Baldwin SA, Young JD. 2011. Nucleobase Transport by Human Equilibrative Nucleoside Transporter 1 (hENT1). *J. Biol. Chem.* 286:32552-62
34. Ritzel MWL, Ng AML, Yao SYM, Graham K, Loewen SK, et al. 2001. Molecular Identification and Characterization of Novel Human and Mouse Concentrative Na+-Nucleoside Cotransporter Proteins (hCNT3 and mCNT3) Broadly Selective for Purine and Pyrimidine Nucleosides (System cib). *J. Biol. Chem.* 276:2914-27
35. Moseley RH, Jarose S, Permoad P. 1991. Adenosine transport in rat liver plasma membrane vesicles. *American Journal of Physiology-Gastrointestinal and Liver Physiology* 261:G716-G22
36. Karsai D, Zsuga J, Juhasz B, Der P, Szentmiklosi AJ, et al. 2006. Effect of nucleoside transport blockade on the interstitial adenosine level characterized by a novel method in guinea pig atria. *Journal of Cardiovascular Pharmacology* 47:103-9
37. Zhang G, Franklin PH, Murray TF. 1993. Manipulation of endogenous adenosine in the rat prepiriform cortex modulates seizure susceptibility. *The Journal of Pharmacology and Experimental Therapeutics* 264:1415-24
38. Gonzalez-Benitez E, Guinzberg R, Diaz-Cruz A, Pina E. 2002. Regulation of glycogen metabolism in hepatocytes through adenosine receptors. Role of Ca2+ and cAMP. *Eur J Pharmacol* 437:105-11
39. Steculorum SM, Paeger L, Bremser S, Evers N, Hinze Y, et al. 2015. Hypothalamic UDP Increases in Obesity and Promotes Feeding via P2Y6-Dependent Activation of AgRP Neurons. *Cell* 162:1404-17
40. Meijer P, Oyen WJ, Dekker D, van den Broek PH, Wouters CW, et al. 2009. Rosuvastatin increases extracellular adenosine formation in humans in vivo: a new perspective on cardiovascular protection. *Arterioscler Thromb Vasc Biol* 29:963-8
41. Wang C, Lin W, Playa H, Sun S, Cameron K, Buolamwini JK. 2013. Dipyridamole analogs as pharmacological inhibitors of equilibrative nucleoside transporters. Identification of novel potent and selective inhibitors of the adenosine transporter function of human equilibrative nucleoside transporter 4 (hENT4). *Biochem Pharmacol* 86:1531-40

42. Ooba N, Tanaka S, Yasukawa Y, Yoshino N, Hayashi H, et al. 2016. Effect of high-potency statins on HbA1c in patients with or without diabetes mellitus. *Journal of Pharmaceutical Health Care and Sciences* 2:8
43. Al-Jibouri LM, Najim RA. 1988. Effect of dipyridamole on blood glucose and liver cyclic amp levels and platelet count during endotoxaemia in mice. *Clinical and Experimental Pharmacology and Physiology* 15:527-32

Figure Legends

Figure 1 – 8CPT-cAMP inhibits the ability of AICAR but not metformin to suppress HGP in primary hepatocytes. **(A)** HGP was measured from primary mouse hepatocytes after 8 hours incubation with or without 8CPT-cAMP (100 μM) in the presence or absence of metformin (Met; 250 μM) or AICAR (250 μM). **(B)** Representative immunoblots of pThr172 AMPK and pSer79 ACC from primary hepatocytes treated with metformin (250 μM), AICAR (250 μM) ± 8CPT-cAMP (100 μM). **(C, D)** provides densitometric analysis of phosphorylation of ACC (C) and AMPK (D), expressed as fold change of control (n=3). All data is expressed as mean +/- SEM and analysed by ANOVA (*p<0.05, ** p<0.01, *** p<0.001). Con = control in this and all other figures.

Figure 2 – Dibutyryl cAMP and glucagon do not inhibit the effect of AICAR on HGP or AMPK signalling. Primary mouse hepatocytes were incubated for 8 hours with either dibutyryl cAMP (db-cAMP; 100 μM) **(A)** or glucagon (100 nM) **(B)** in the presence or absence of metformin (Met; 250 μM) or AICAR (250 μM). The amount of glucose produced was measured as in Fig. 1A. **(C)** Immunoblots showing pT172 AMPK and pS79 ACC phosphorylation in response to db-cAMP (100 μM). **(D, E)** provides densitometric analysis of phosphorylation of ACC (D) and AMPK (E), expressed as fold change of control. Data is expressed as mean +/- SEM from three separate experiments and analysed by ANOVA (*p<0.05, ** p<0.01, *** p<0.001 in pairwise differences).

Figure 3 – Suppression of HGP and AMPK signalling by AICAR is inhibited by the 8CPT-modified cAMP analogue 8CPT-2-Methyl-O-cAMP. Primary hepatocytes were treated for 8 hours with metformin (Met; 250 μM) or AICAR (250 μM) ± 8CPT-2MeO-cAMP (100 μM) **(A).** Media was harvested and HGP measured

as in Fig. 1 A (n=4). **(B)** Representative immunoblots of pThr172 AMPK and pSer79 ACC phosphorylation in lysates treated with metformin (Met; 250 μM) or AICAR (250 μM) ± 8CPT-2MeO-cAMP (100 μM). **(C-F)** provides densitometric analysis of ACC (C, E) and AMPK (D, F) phosphorylation, expressed as fold change of control (n=4). Data is expressed as mean +/- SEM and analysed by ANOVA (*p<0.05, ** p<0.01, *** p<0.001 in pairwise comparisons).

Figure 4 - AICAR uptake into hepatocytes is mediated by equilibrative nucleoside transporter 1 (ENT1). (A) HGP was measured after incubation for 8 hours with the selective ENT1 inhibitor NBMPR (100 nM) ± metformin (250 μM) or AICAR (250 μM). The amount of glucose produced was normalised to protein content and expressed as % control. **(B)** Representative immunoblots measuring pThr172 AMPK and pSer79 ACC by metformin (250 μM) or AICAR (250 μM) ± NBMPR (100 nM). **(C-F)** provides densitometric analysis of ACC (C, E) and AMPK (D, F) phosphorylation, expressed as fold change of control. Data is taken from 4 separate experiments and shown as mean +/- SEM, (*p<0.05 ** p<0.01, *** p<0.001 in pairwise comparisons, 'ns' denotes not significant).

Figure 5 - Nucleoside transport via equilibrative nucleoside transporter 1 (ENT1) is inhibited by 8CPT-modified cAMP analogues. Uridine uptake into hepatocytes was measured using ^{3}H-uridine uptake assay. Hepatocytes were incubated for 15 minutes with NBMPR (100 nM), 8CPT-cAMP (100 μM), Dibutyryl cAMP (100 μM), glucagon (100 nM) or 8CPT-2MeO-cAMP (100 μM) before measuring ^{3}H transport into the cell for one minute. Data is expressed as mean +/- SEM and is represented as % uridine uptake relative to control. (n=3; **p<0.01, *** p<0.001; NS denotes not significant). (B) LC-MS analysis of AICAR in medium without cells at zero time and 6h incubation. The top two traces show the similarity

between total MS signal at zero time and 6h incubation. The bottom two traces show the signal at the selected *m/z* 259 for AICAR and demonstrate that AICAR is effectively stable under these conditions. The full-scale deflection of the MS detector is given in the top right corner of each trace. (C) AICAR disappearance from medium in the presence of primary hepatocytes. AICAR in media was measured by LC-MS and expressed as μM AICAR. Data is expressed as mean +/- SEM and analysed by ANOVA (*p<0.05 in pairwise comparisons). (D) Effect of NBMPR, 8CPT-cAMP and 2MeO-8CPT-cAMP on AICAR disappearance from the medium. AICAR in media was measured by LC-MS and expressed as peak areas in MS detector units. Data is expressed as mean +/- SEM and analysed by ANOVA ((*p<0.05 & ** p<0.01 in pairwise comparisons)).

(E) Schematic representation of AICAR and metformin entry into hepatocytes and consequences of equilibrative nucleoside transporter (ENT1) inhibition. *Upper section:* AICAR enters the hepatocyte through ENT1, where it is converted to AICAR monophosphate (ZMP), resulting in suppression of HGP through AMPK-independent targets. Metformin enters hepatocytes at least in part through organic cationic transporters (OCT) and inhibits HGP through mechanisms including mitochondrial inhibition affecting adenine nucleotide levels/ratios. *Lower section:* NBMPR inhibits adenosine uptake into hepatocytes through ENT1, raising HGP which is possibly mediated, at least in part, by an adenosine receptor (Adora)-mediated process.

Figure 1

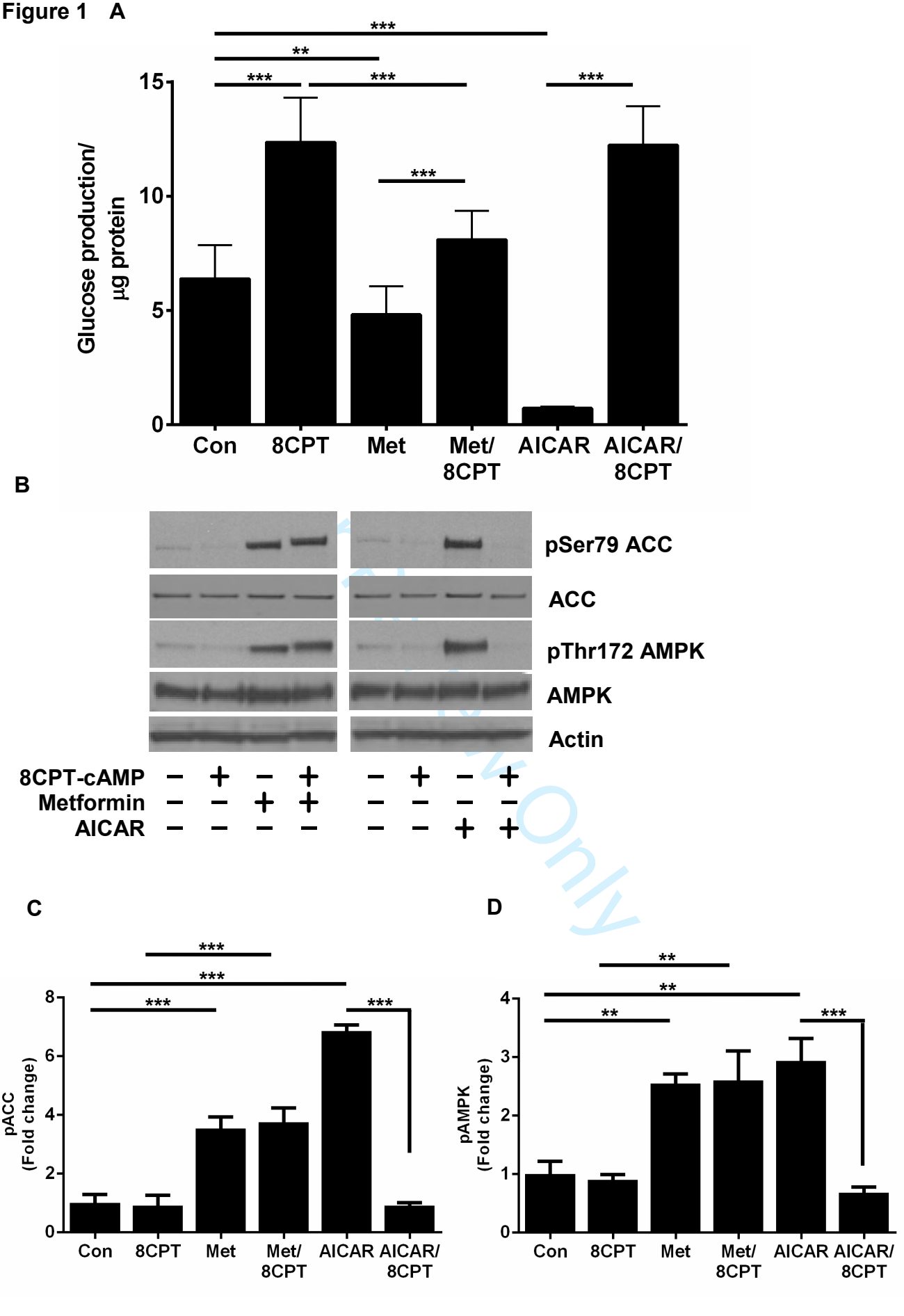

Figure 2

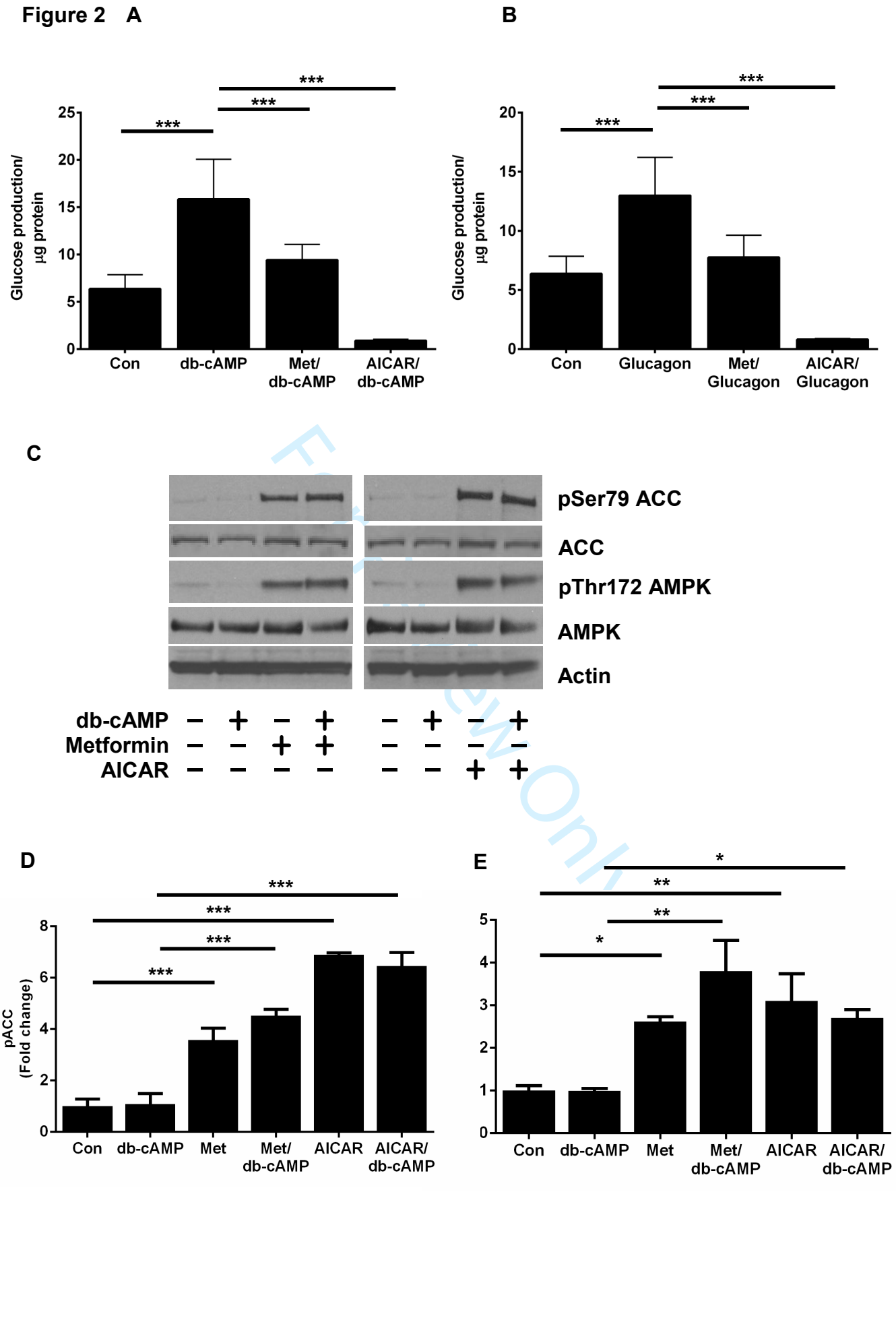

Figure 3

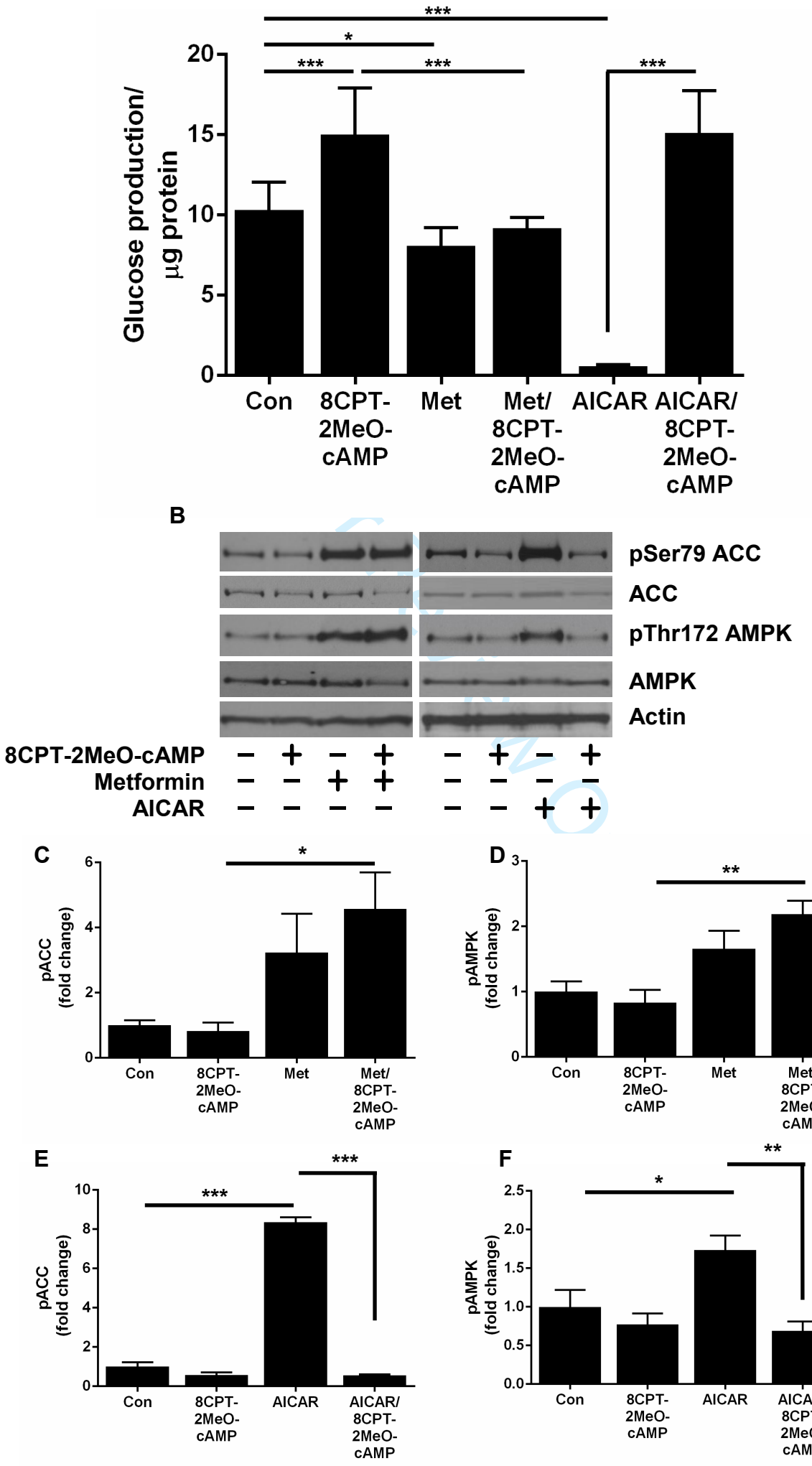
A
Glucose production/ µg protein
Con
8CPT-2MeO-cAMP
Met
Met/ 8CPT-2MeO-cAMP
AICAR
AICAR/ 8CPT-2MeO-cAMP
B
pSer79 ACC
ACC
pThr172 AMPK
AMPK
Actin
8CPT-2MeO-cAMP
Metformin
AICAR
C
pACC (fold change)
D
pAMPK (fold change)
E
pACC (fold change)
F
pAMPK (fold change)

Figure 4 A

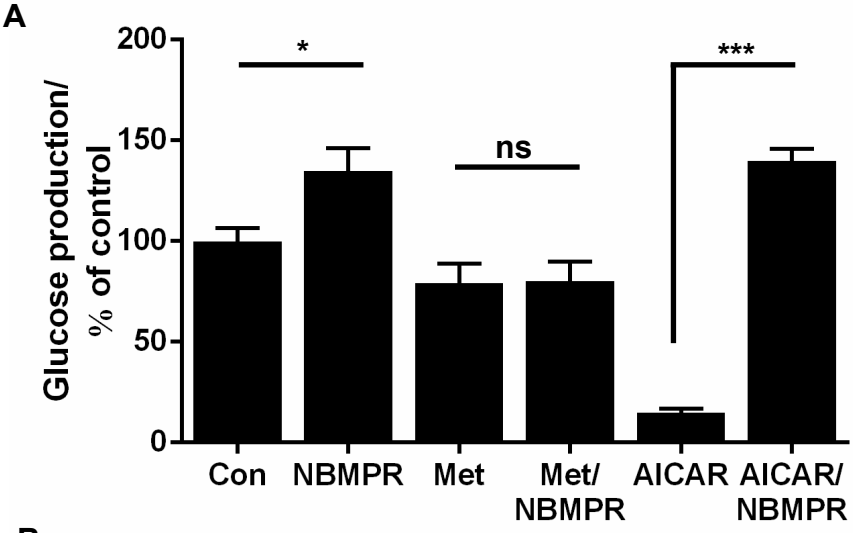

B

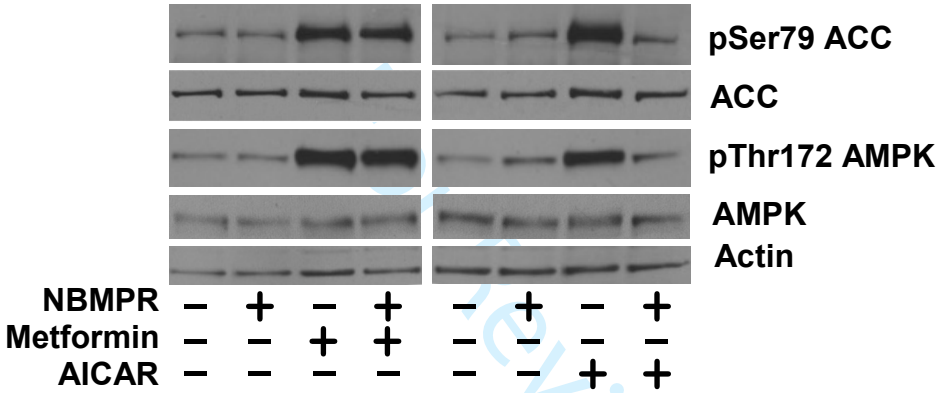

C

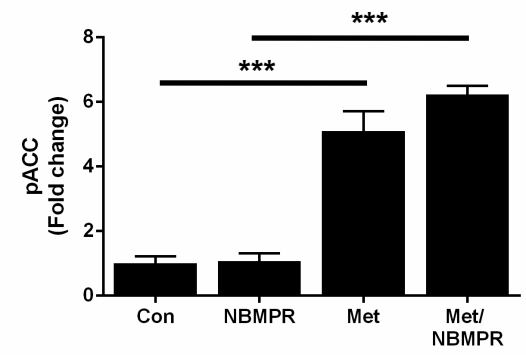

D

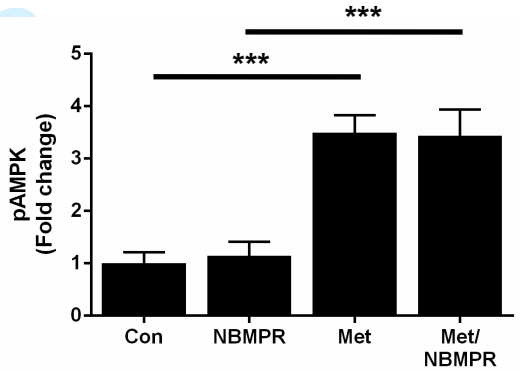

E

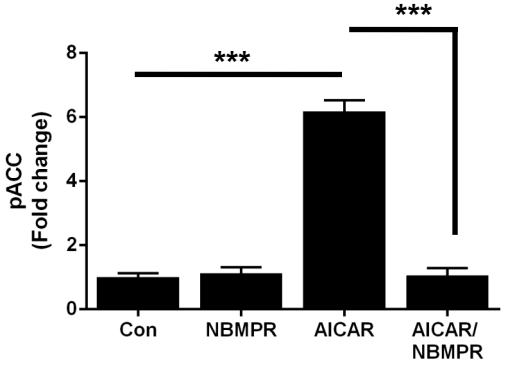

F

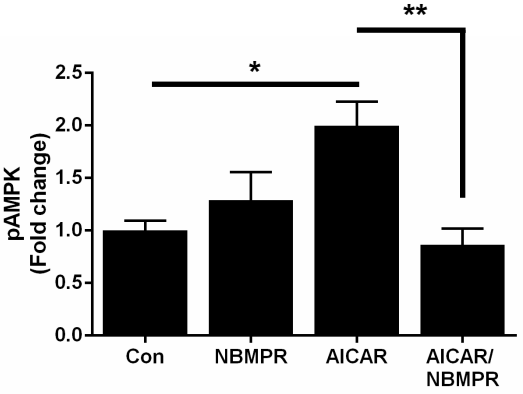

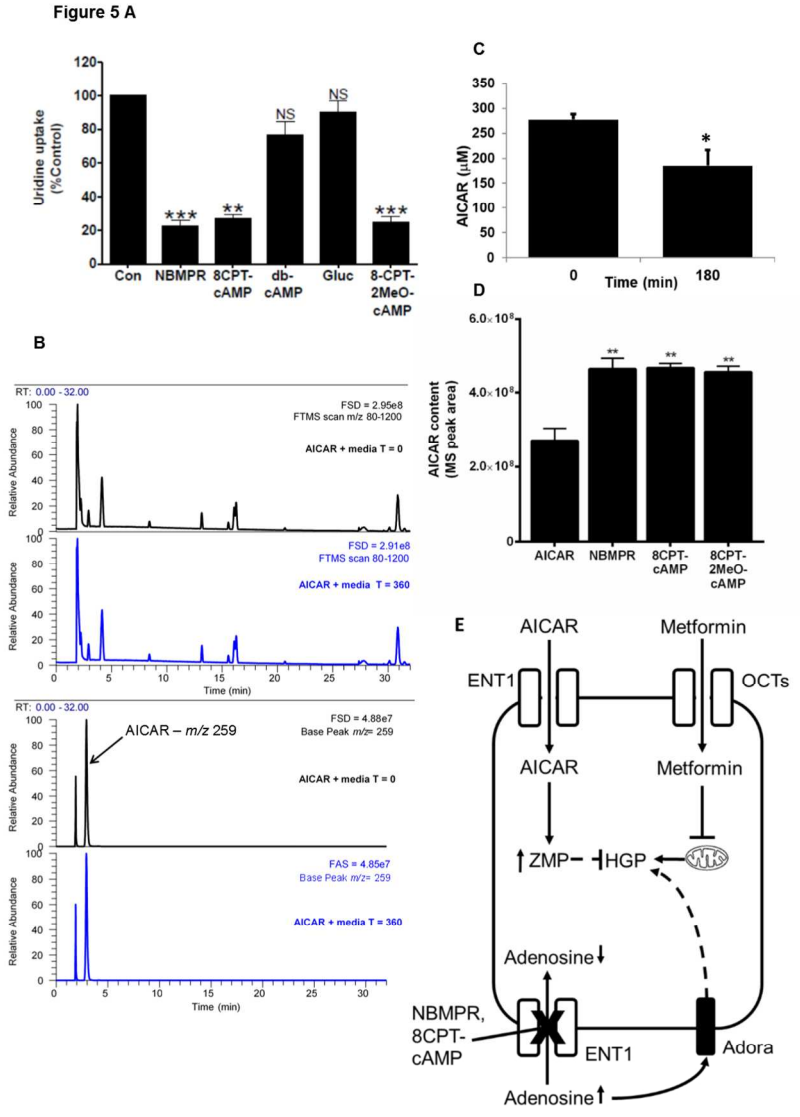

209x297mm (150 x 150 DPI)